

Burridge-Knopoff model and self-similarity

P.G.Akishin¹, M.V.Altaisky^{1,2}, I.Antoniou^{3,4}, A.D.Budnik¹, V.V.Ivanov^{1,3}

¹ *Laboratory of Computing Techniques and Automation, Joint Institute for Nuclear Research, Dubna, 141980, RUSSIA*

² *Space Research Institute RAS, Profsoyuznaya 84/32, Moscow, 117810, RUSSIA*

³ *International Solvay Institute for Physics and Chemistry, CP-231, ULB, Campus Plaine, Bd. du Triomphe, 1050, Brussels, BELGIUM*

⁴ *Theoretische Natuurkunde, Free University of Brussels, Brussels, BELGIUM*

The seismic processes are well known to be self-similar in both spatial and temporal behavior. At the same time, the Burridge-Knopoff (BK) model of earthquake fault dynamics, one of the basic models of theoretical seismology, does not possess self-similarity. In this article an extension of BK model, which directly accounts for the self-similarity of earth crust elastic properties by introducing nonlinear terms for inter-block springs of BK model, is presented. The phase space analysis of the model has shown it to behave like a system of coupled randomly kicked oscillators. The nonlinear stiffness terms cause the synchronization of collective motion and produce stronger seismic events.

I. INTRODUCTION

The earthquake – a sudden stress relief in earth crust – is believed to take place when and where the stress exceeds certain critical value. At the same time, it is well known that the rock materials are not continuous in physical sense: they consist of grains or crystals of different sizes separated from each other by cracks of all possible sizes. The picture is more or less the same from the typical grain sizes up to the external size of the seismic zone. The situation very much resembles that in developed turbulence, described by Kolmogorov [Kol41a]. Therefore, we have to deal with a system with well manifested self-similarity properties. The self-similarity of seismic processes has got a lot of attention in phenomenological studies (see e. g. [Kag94,KB94] and references therein). A theoretical account for self-similarity of earth crust fracturing was given by Newman and Knopoff [NK90,Kol41b] and some other authors on the base of renormalization approach. The dynamical modeling of self-similar velocity weakening friction in BK model was recently presented in [SVR96]. Their hierarchical BK model accounts for cascade rupture propagation and seems to give a simple explanation to the Coulomb friction law so widely observed in nature. However, their model does not account for nonlinear elasticity which is also significant for earth crust deformations [ZL95].

The crux of our paper is the direct account of self-similarity (and scale-dependence, as it will be shown below) in the spirit of self-similar elasticity [ZL95]. Taking self-similarity as a given property of the rock material, we have changed the harmonic springs ($U = \frac{kx^2}{2}$) in BK model [BK67] to nonlinear ones possessing self-similarity (to be explained below). We compare our simulations with that of standard BK model [CL89,SVR93] and found our model to be more realistic in the sense of foreshocks and aftershocks clustering [Ger93]. Besides that, the nonlinear elasticity, which we have yielded from the self-similarity, leads to the nonlinear stiffness of the form

$$f(x) = -k(x)x, \quad \text{where} \quad k(x) = k_0 \left[1 + \epsilon \left(\frac{x}{a} + \frac{x^2}{2a^2} \right) + \dots \right],$$

where a is the length of relaxed spring. This nonlinearity is adequate to well known empirical fact of nonlinear stiffness of the crust.

The remainder of this paper is organized as follows. In *section 2* we remind the original BK model and analyze its virtues and shortcomings. The self-similar stiffness modification of BK model is presented in *section 3*. *Section 4* is devoted to the numerical algorithm used for simulations. In *section 5* we compare our model and the original Burridge-Knopoff one. The statistical characteristics – autocorrelation function and the Hurst exponent – are also presented here. In *section 6* we give some dynamical analysis of the model, which shows that the BK system behaves like a system of kicked oscillators.

II. THE BURRIDGE-KNOPOFF MODEL

There is no mechanical model capable of simulating all the features of real seismic process. However, to study the temporal characteristics of earthquake dynamics is sufficient to isolate a few main properties of the process. The feature isolated and put as a basis for the mechanical model of earthquakes was a conjecture that earthquake faults are

retarded by nonlinear friction between blocks of rock material. Such a purely dynamical model obeying the Newton laws, without any *ad hoc* taken random forces, has been proposed by R. Burridge and L. Knopoff 30 years ago [BK67].

The BK system is a system of N blocks of mass m_i , $i = \overline{1, N}$ rested on a rough surface and connected by harmonic springs of stiffness k_c to each other; each block is attached by a leaf spring of stiffness k_p to moving upper line, see Fig. 1.

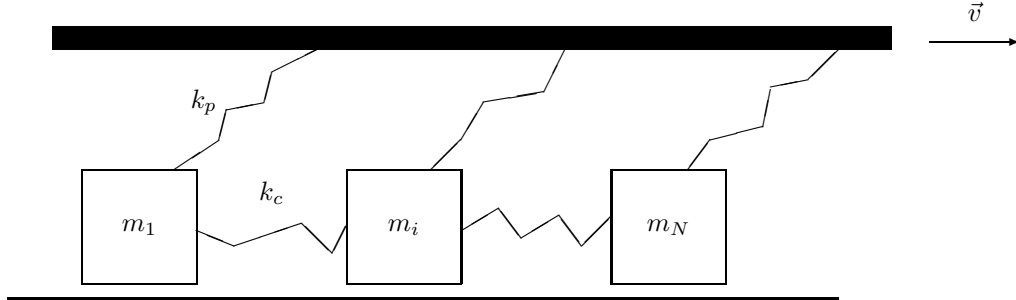


FIG. 1. The geometry of the BK model: the system is composed of N identical blocks of mass m_i , k_c is the stiffness of “horizontal” springs, k_p is the stiffness of pulling springs, v is the constant velocity of pulling line.

Initially (at $t = 0$) the system is at rest, and the elastic energy accumulated in “horizontal” springs is only due to randomly generated small initial displacements of the blocks from their neutral positions. The moving upper line, which simulates the movement of external driving plate, exerts the force $f_n = -k_p(x_n - vt)$ on each n -th block. The nonlinear friction is defined in such a way that it holds each block at rest until the sum of all forces applied to this block exceeds certain critical value F_0 . Then the block makes a slip inhibited by nonlinear friction to a new position. A pause between two slips is believed to account for a pause between earthquakes.

Despite its simplicity, the BK model enables to simulate sequences of slipping events, similar to that of real earthquakes. The distribution of event size, generated by BK model also resembles the Gutenberg-Richter power law [GR44]. However, for practical purposes of generating artificial earthquake catalogs, the “reliability” of BK toy model is not always sufficient. A number of attempts have been made to modify BK model to gain more realistic sequences of events, to gain more sharp clusterization first of all [Ger93].

Following [CL89] we rewrite the equations of motion in using dimensionless coordinates:

$$\ddot{u}_n = l^2(u_{n+1} - u_n) + l^2(u_{n-1} - u_n) - u_n + \nu\tau + F(\dot{u}_n), \quad (1)$$

where $u_n = \frac{k_p x_n}{F_0}$ is normalized displacement, $l = \sqrt{k_c/k_p}$ is normalized sound velocity, $\nu = \frac{vk_p}{\omega_p F_0}$ is dimensionless driving velocity, F_0 is the amplitude of friction force. The upper dots denote differentiation with respect to dimensionless time $\tau = \omega_p t$, $\omega_p^2 = \frac{k_p}{m}$. The adimensional version of friction force [BK67] is taken in the form

$$F(\dot{u}) = \begin{cases} -\frac{u}{H} & \text{for } |\dot{u}| \leq H \\ -\frac{F_0}{1+D(\dot{u}-H)} - E(\dot{u}-H) & \text{for } \dot{u} > H \\ +\frac{F_0}{1-D(\dot{u}+H)} - E(\dot{u}+H) & \text{for } \dot{u} < -H \end{cases}, \quad (2)$$

where E is a linear friction coefficient, H is a threshold velocity below which blocks can move without causing fracture effects; D is a parameter of friction nonlinearity.

To keep with [BK67,CL89] we have chosen $E = F_0 = k_p = m = 1$, $D = 5$, $\nu = 0.01$. The velocity threshold value was taken $H = 0.001$. We have performed simulations for 10, 50 and 100 blocks chains.

The BK system has several evident time scales. The characteristic time $T_p = \omega_p^{-1}$ is the typical time of harmonic oscillation; $\tau_L = 1/\nu$ (dimensionless units) is the time taken by driving force $u - \nu\tau$ to reach the critical value $F_0 = 1$ and to cause a slip; $\tau_s = N/l$ is the time required by a “sound” wave traveling with velocity l to pass over entire chain of N blocks. The ratio of the two latter parameters $\theta = \frac{N\nu}{l}$ is an important parameter of the system, which accounts for the transition from chaotic to solitary wave regime [SVR93,SVR96]. However, in the discrete spring-block model (1) there is no dependence on the relaxed spring length a . It seems natural on one hand – the seismic processes are scale-invariant practically at all scales, – but on the other hand the model admits the possibility of block overlapping, when simulated numerically. The latter is completely unphysical.

III. SCALE DEPENDENT BK MODEL

A. Scale invariant stiffness model

Regardless all the merits of spring-block model evidently it does not adequately describe the elastic properties of rock material.

Let us consider a spring of relaxed length a . If we contract or dilate it by Δx , we exhibit a reaction force $f = -k\Delta x$; where k is its stiffness. However, it is absolutely impossible to contract a spring up to zero length, $\Delta x = a$. More than that, as any geologist knows, in practice k is not the same for large contractions and dilations. More precisely, the stiffness monotonously decreases when going from contractions to dilations, and then, achieving certain critical value, rock crashes.

The simplest way to describe such behavior is to add cubic and quartic terms to spring potential energy

$$U(\Delta x) = \frac{k(\Delta x)^2}{2} + A(\Delta x)^3 + B(\Delta x)^4.$$

However, since we are going to deal with earthquake processes, we also have to account for such a well manifested property of the crust as self-similarity. Following [ZL95], let us take the stiffness to be homogeneous of degree ϵ

$$k(\lambda l) = \lambda^{-\epsilon} k(l), \quad (3)$$

normalized to the rigidity of relaxed spring $k(a) = k_0$. The energy of the finite deformation Δx is then given by

$$U(\Delta x) = \int_0^{\Delta x} k(y)y dy = \int_0^{\Delta x} \frac{a^\epsilon k_0 y dy}{(a-y)^\epsilon}. \quad (4)$$

After straightforward calculation this gives

$$U(u) = k_0 a^2 \left[\frac{1}{1-\epsilon} (1 - (1-u)^{1-\epsilon}) - \frac{1}{2-\epsilon} (1 - (1-u)^{2-\epsilon}) \right], \quad (5)$$

where $u = \frac{\Delta x}{a}$ is the relative deformation. The graph of the function $U(u)$ is presented in Fig. 2.

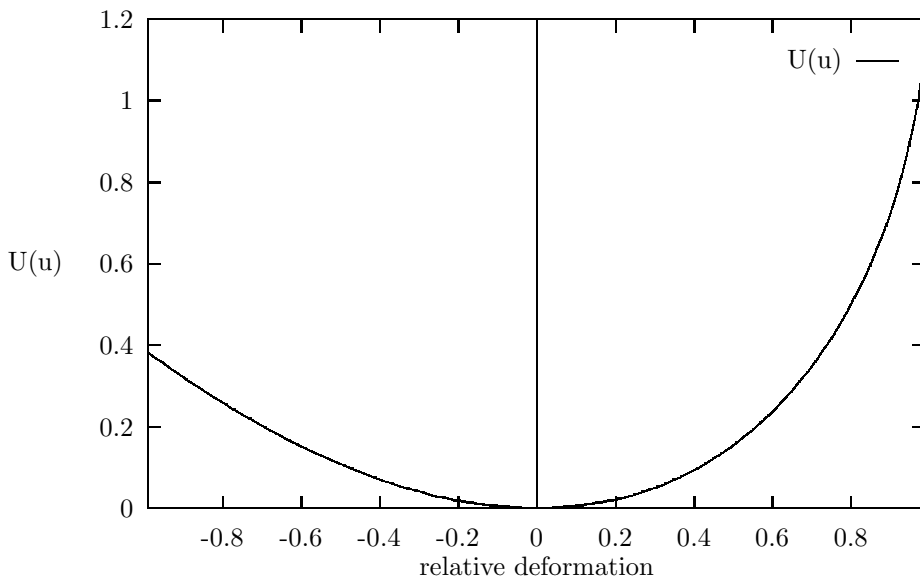


FIG. 2. The graph of the potential energy of a spring with self-similar stiffness $k(\lambda a) = \lambda^{-\epsilon} k(a)$, function (5). X-axis values correspond to relative deformation $u = \frac{\Delta x}{a}$, where a is the length of relaxed spring. Plotted for $\epsilon = 0.5$, $k_0 = a = 1$.

We will proceed with a case of small nonlinearity, which is the restriction of general formula (5) for the case of small ϵ , and has convenient linear stiffness $k = \text{const}$ as a limiting case at $\epsilon \rightarrow 0$. We will concentrate ourselves on elastic nonlinearity without taking friction into account at this point. Taking the Taylor expansion of (5) with respect to ϵ

$$U(u) = k_0 a^2 \left[\frac{u^2}{2} + \epsilon \left(\frac{u^3}{3} + \frac{u^4}{8} + \frac{u^5}{15} \right) + \epsilon^2 \left(\frac{u^4}{8} + \frac{u^5}{10} \right) + o(\epsilon^3) \right]. \quad (6)$$

In the first order with respect to ϵ we get $f(x) = -\frac{\partial U}{\partial x} = -k_1(x)x$, where

$$k_1(x) = k_0 \left[1 + \epsilon \left(\frac{x}{a} + \frac{x^2}{2a^2} + \frac{x^4}{3a^3} \right) \right]$$

is the deformation dependent spring strength. Therefore, the self-similarity of elastic media necessarily causes nonlinearity.

Using the nonlinear potential (6) for small displacements ($u \ll 1$) we have

$$U(u) = k_0 a^2 \left[\frac{u^2}{2} + \epsilon \left(\frac{u^3}{3} + \frac{u^4}{8} \right) + o(\epsilon^2) \right], \quad (7)$$

as a spring potential, we account for small influence of self-similar stiffness ($\epsilon \ll 1$).

The first term of the equation (7), the harmonic spring potential, is already contained in the BK model. The nonlinearity comes from the second term. The force applied to the n -th block of the spring-block chain due to this nonlinear term is

$$f_{nlin}(x_n) = -\frac{\partial}{\partial x_n} U_{nlin}, \quad U_{nlin} = \sum_n \frac{k_c \epsilon}{3a} \Delta_n^3 + \frac{k_c \epsilon}{8a^2} \Delta_n^4, \quad (8)$$

where $\Delta_n = x_n - x_{n+1}$. So, the nonlinear stiffness term will appear at the r. h. s. of equation of motion (1):

$$m\ddot{x}_n = k_c(x_{n+1} - 2x_n + x_{n-1}) - k_p(x_n - vt) + f_{nlin}(x_n) + \hat{F}(\dot{x}_n),$$

where $f_{nlin}(x_n)$, given by (8). In dimensionless form the spring-block equation (1) with nonlinear terms described above takes the form

$$\begin{aligned} \ddot{u}_n &= l^2(u_{n+1} - u_n) - l^2(u_n - u_{n-1}) - u_n + \nu\tau \\ &+ \alpha [(u_{n+1} - u_n)^2 - (u_n - u_{n-1})^2] \\ &+ \beta [(u_{n+1} - u_n)^3 - (u_n - u_{n-1})^3] + F(\dot{u}_n), \end{aligned} \quad (9)$$

where the dimensionless nonlinearity parameters are

$$\alpha = -\frac{l^2 \epsilon F_0}{ak_p}, \quad \beta = \frac{l^2 \epsilon F_0^2}{2a^2 k_p^2};$$

all other notations are the same as for the equation (1).

IV. NUMERICAL IMPLEMENTATION

In this section we consider the Burridge-Knopoff model consisting on N blocks. For numerical simulations we rewrite equation (1) separately for boundary ($i = 1, N$) and internal blocks ($1 < i < N$) motion in the following form:

$$\begin{aligned} \ddot{x}_1 &= l^2(x_2 - x_1) - (x_1 - \nu t) + \Psi_1(x_1, x_2, \dot{x}_1), \\ \ddot{x}_N &= l^2(x_{N-1} - x_N) - (x_N - \nu t) + \Psi_N(x_N, x_{N-1}, \dot{x}_N), \\ \ddot{x}_i &= l^2(x_{i-1} - 2x_i + x_{i+1}) - (x_i - \nu t) + \Psi_i(x_{i-1}, x_i, x_{i+1}, \dot{x}_i), \\ &\quad i = 2, \dots, N-1, \end{aligned} \quad (10)$$

where functions Ψ_i comprise nonlinear terms of r. h. s. of (1). Free boundary conditions were set for the first and the last blocks.

The problem is reduced to the solution of the nonlinear equations of motion (10) with given initial conditions:

$$x_i(t_0) = u_i^0, \quad \dot{x}_i(t_0) = v_i^0, \quad i = 1, \dots, N. \quad (11)$$

Let $p_i(t) = \dot{x}_i(t)$. We rewrite the system (10,11) in the following form:

$$\begin{aligned} \dot{x}_i &= p_i(t), \quad i = 1, \dots, N, \\ \dot{p}_1 &= l^2(x_2 - x_1) - (x_1 - \nu t) + \Psi_1(x_1, x_2, p_1), \\ \dot{p}_N &= l^2(x_{N-1} - x_N) - (x_N - \nu t) + \Psi_N(x_N, x_{N-1}, p_N), \\ \dot{p}_i &= l^2(x_{i-1} - 2x_i + x_{i+1}) - (x_i - \nu t) + \Psi_i(x_{i-1}, x_i, x_{i+1}, p_i), \\ & \quad i = 2, \dots, N-1, \end{aligned} \quad (12)$$

with initial conditions:

$$x_i(t_0) = u_i^0, \quad p_i(t_0) = v_i^0, \quad i = 1, \dots, N. \quad (13)$$

This scheme has been used for numerical simulations of both linear BK model ($\epsilon = 0$) and that with nonlinear terms ($\epsilon > 0$). The nonlinear friction was given by (2). The initial displacements u_i were randomly generated with the amplitude 0.0001, the initial velocities were set to zero, we choose $l^2 = 100$. Let δt be the time step $t_l = t_0 + l\delta t$. To get an approximate solution of the Cauchy problem (12, 13) we use the implicit numerical scheme:

$$\begin{aligned} \frac{x_i^l - x_i^{l-1}}{\delta t} &= 0.5(p_i^l + p_i^{l-1}), \quad i = 1, \dots, N, \\ \frac{(p_1^l - p_1^{l-1})}{\delta t} &= 0.5(l^2(x_2^l - x_1^l) - x_1^l + l^2(x_2^{l-1} - x_1^{l-1}) - x_1^{l-1}) \\ & \quad + \nu t + \Psi_1(x_1^{l-1}, x_2^{l-1}, p_1^{l-1}), \\ \frac{(p_N^l - p_N^{l-1})}{\delta t} &= 0.5(l^2(x_{N-1}^l - x_N^l) - x_N^l + l^2(x_{N-1}^{l-1} - x_N^{l-1}) - x_N^{l-1}) \\ & \quad + \nu t + \Psi_N(x_N^{l-1}, x_{N-1}^{l-1}, p_N^{l-1}), \\ \frac{(p_i^l - p_i^{l-1})}{\delta t} &= 0.5(l^2(x_{i-1}^l - 2x_i^l + x_{i+1}^l) - x_i^l + l^2(x_{i-1}^{l-1} - 2x_i^{l-1} + x_{i+1}^{l-1}) - x_i^{l-1}) \\ & \quad + \nu t + \Psi_i(x_{i-1}^{l-1}, x_i^{l-1}, x_{i+1}^{l-1}, p_i^{l-1}), \quad i = 2, \dots, N-1, \end{aligned} \quad (14)$$

with initial conditions (13). To keep with [BK67,CL89] we have chosen $E = F_0 = k_p = m = 1, D = 5, \nu = 0.01$. The velocity threshold value was taken $H = 0.001$.

V. RESULTS

A. General outlook

The dynamical behavior of both linear (1) and nonlinear (10) models was studied in terms of potential and kinetic energy. We calculated the time dependence of potential U and kinetic T energies:

$$\begin{aligned} U_c(\tau) &= \frac{l^2}{2} \sum_{i=1}^{N-1} (u_{i+1}(\tau) - u_i(\tau))^2, \\ & \quad - \frac{l^2\epsilon}{3} \sum_{i=1}^{N-1} (u_{i+1}(\tau) - u_i(\tau))^3 + \frac{l^2\epsilon}{8} \sum_{i=1}^{N-1} (u_{i+1}(\tau) - u_i(\tau))^4, \\ U_m(\tau) &= \frac{1}{2} \sum_{i=1}^N (\nu\tau - u_i(\tau))^2, \end{aligned} \quad (15)$$

$$U_{pot} = U_c + U_m,$$

$$T(\tau) = \frac{1}{2} \sum_{i=1}^N \dot{u}_i^2(\tau). \quad (16)$$

The dependence of the energies on dimensionless time τ is shown in Figs. 3 and 4, for linear ($\epsilon = 0$) and nonlinear ($\epsilon = 0.2$) model, respectively.

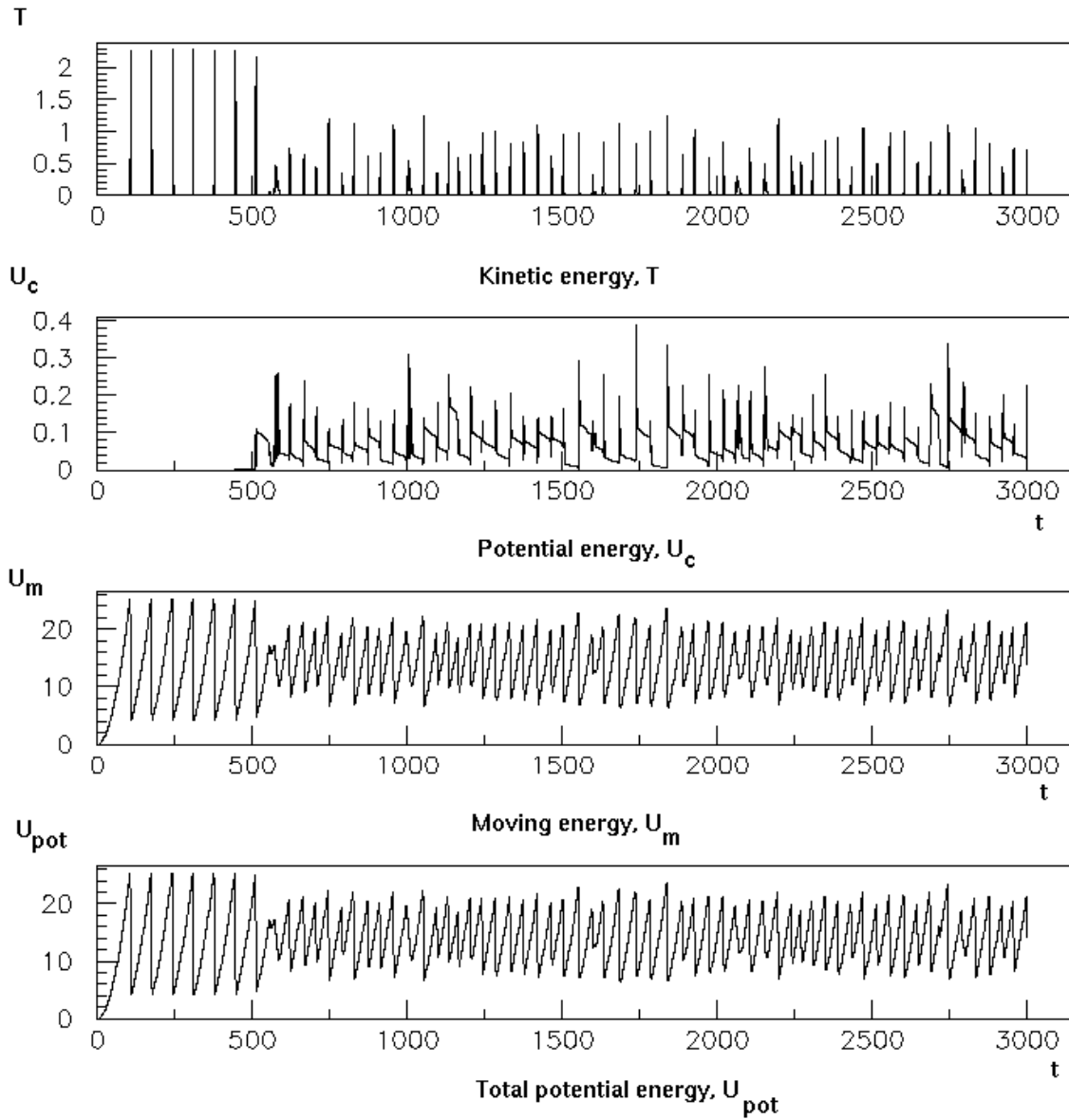


FIG. 3. Potential and kinetic energies for the linear ($\epsilon = 0$) $N=100$ block BK system $l = 10, F_0 = 1, D = 5, H = 0.001, E = 1$.

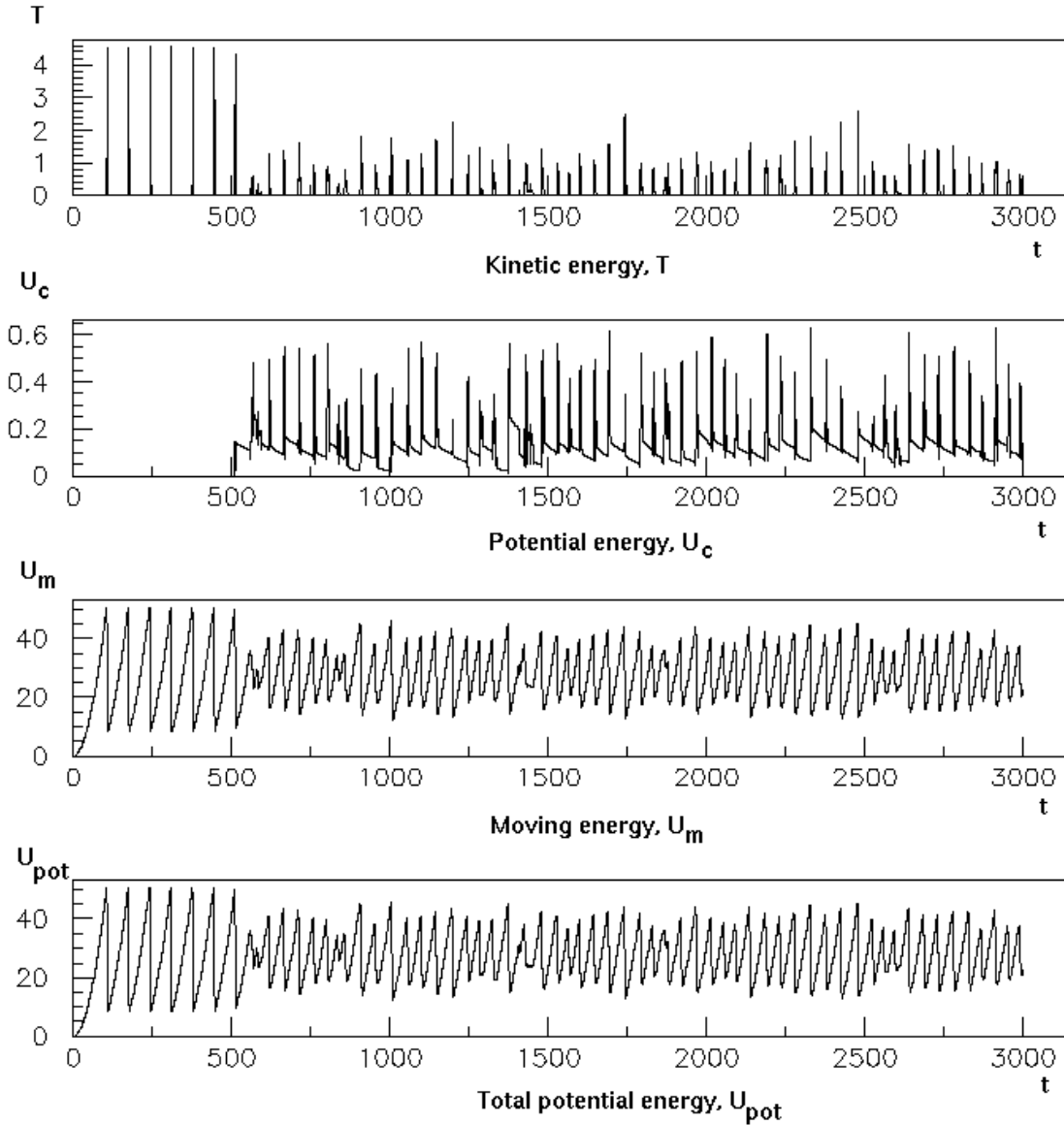


FIG. 4. Potential and kinetic energies for the nonlinear ($\epsilon = 0.2$), $N=100$ block BK system $l = 10, F_0 = 1, D = 5, H = 0.001, E = 1$.

As it can be seen from the pictures, after the initial period of periodic slip-stick motion of the system as a whole (the typical period of one cycle is about loading time $\tau_L = 1/\nu$, $\tau_L = 100$ for our simulations), the process becomes unstable and the system enters the chaotic regime.

As it was shown in the original paper of R. Burrige and L. Knopoff, the spring block system described by the equation (1) has a trivial solution $\forall n : u_n(t) = \nu t + F(\nu)$. This solution is unstable with respect to small perturbations. The time of instability of this uniform motion is comparable to the loading time τ_L , after which the system exerts a slip.

In our numerical investigations we have found another type of instability. After a period of time the quasi-periodic motion, when the system slides and sticks as a whole, also becomes unstable and actually chaotic when most part of inter-block springs are exited starts. The typical time of this instability is approximately the same for both linear and nonlinear models, see Figs. 3 and 4. At this stage ($\tau < 500$) the inter-block springs k_c have not accumulated

enough energy and the dynamic of the system is determined by nonlinear friction force. Later, when nonlinear terms have got sufficient energy and the role of cubic and quartic terms in (10) becomes significant, the nonlinear model shows stronger clusterization of events than the linear one. This fact was traced on the autocorrelation function (see Fig. 5.),

$$r(z) = \frac{\langle x(t)x(t+z) \rangle}{\langle x^2(t) \rangle}. \quad (17)$$

The averaging was taking over the available time series of energies $0 \leq \tau \leq 2000$. The increasing of correlations at intermediate times ($z < 3\tau_L$) is clearly observed for nonlinear model.

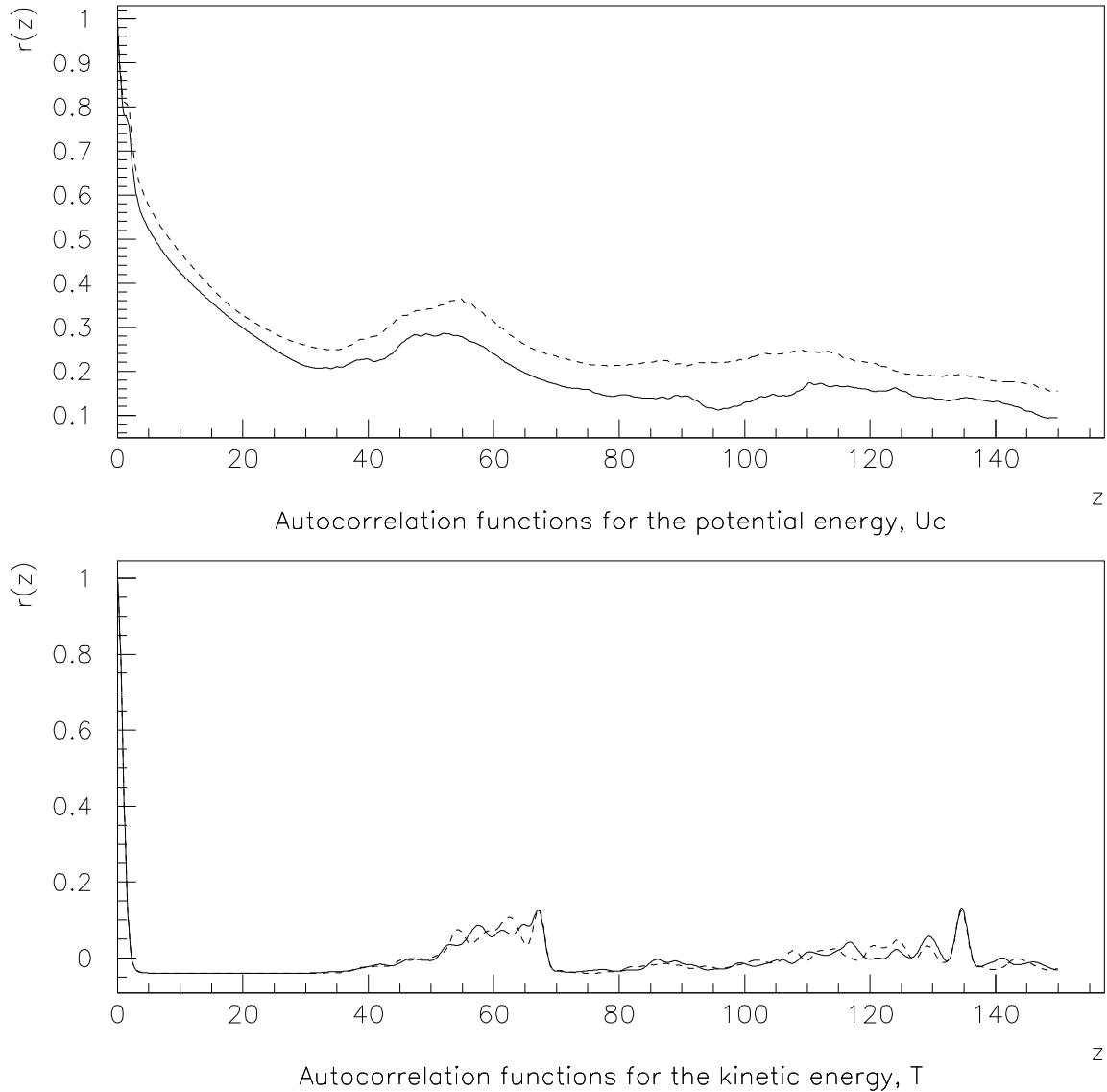


FIG. 5. Autocorrelation functions for potential and kinetic energies. Shown for the nonlinear $\epsilon = 0.1$, (dashed line) and linear models. $N = 10$ blocks for both curves

This leads to a collective behavior and probably provides an inverse energy cascade – an energy flux from high

frequency modes to low frequency ones, like that observed, say, in hydrodynamic turbulence. Besides that we can say the system to mimic *the liquification* processes, taken place for real earthquakes. For strong earthquakes, long before the main earthquake event the foreshock motion of the crust are governed by elasticity equation; later – in co-seismic stage – we have more rheological behavior rather than elastic process. The gravity waves like that on shallow water can be observed on the ground. The origin of these phenomena is that after a period of foreshocks the crust becomes less connected, less continuous and behaves as a system of particles with Van-der-Vaals interaction [Lom94]. In this sense, the instability we have observed at τ about 1000 ($\nu = 0.01, N = 10$) is a solid-liquid phase transition, see Figs. 3,4.

B. Clusterization

The time dependence of potential and kinetic energies (15,16) for linear ($\epsilon = 0$) and non-linear ($\epsilon = 0.2$) model are presented on Figs. 3 and 4, respectively.

The nonlinear potential terms (7) contributes to “horizontal” spring energies (second graph on both pictures). This potential terms, being relatively small in absolute values, play an essential role in nonlinear effects, happening in the spring-block chain. Initially, up to the time $t < 500$, the systems (both linear and non-linear) make a periodic slip-stick behavior as a whole. The potential energy of horizontal springs is very low at this stage: the internal degrees of freedom are not yet activated. Approximately at $\tau = 500$ this periodic motion breaks down to quasi-periodic weakly chaotic regime.

At this stage the nonlinear system shows stronger clusterization, than its linear counterpart; the groups of events looks more distinguished for nonlinear system, see Fig. 4.

It can be seen from both potential energy of “horizontal” springs and the total potential energy (the graphs in the bottom). Possibly, for some other values of parameters a stronger intermittency will be observed. This, however, will be the subject of further investigation. Here we have just to note that nonlinear terms provide more coherence of seismic events (which can be observed as long wave modulation) and make the events stronger since more potential energy is accumulated.

C. Solitons

The dependence of displacement of coordinate and velocity as function of time and number of blocks for the case of nonlinear model $\epsilon = 0.1, N = 10$ is presented on Fig. 6.

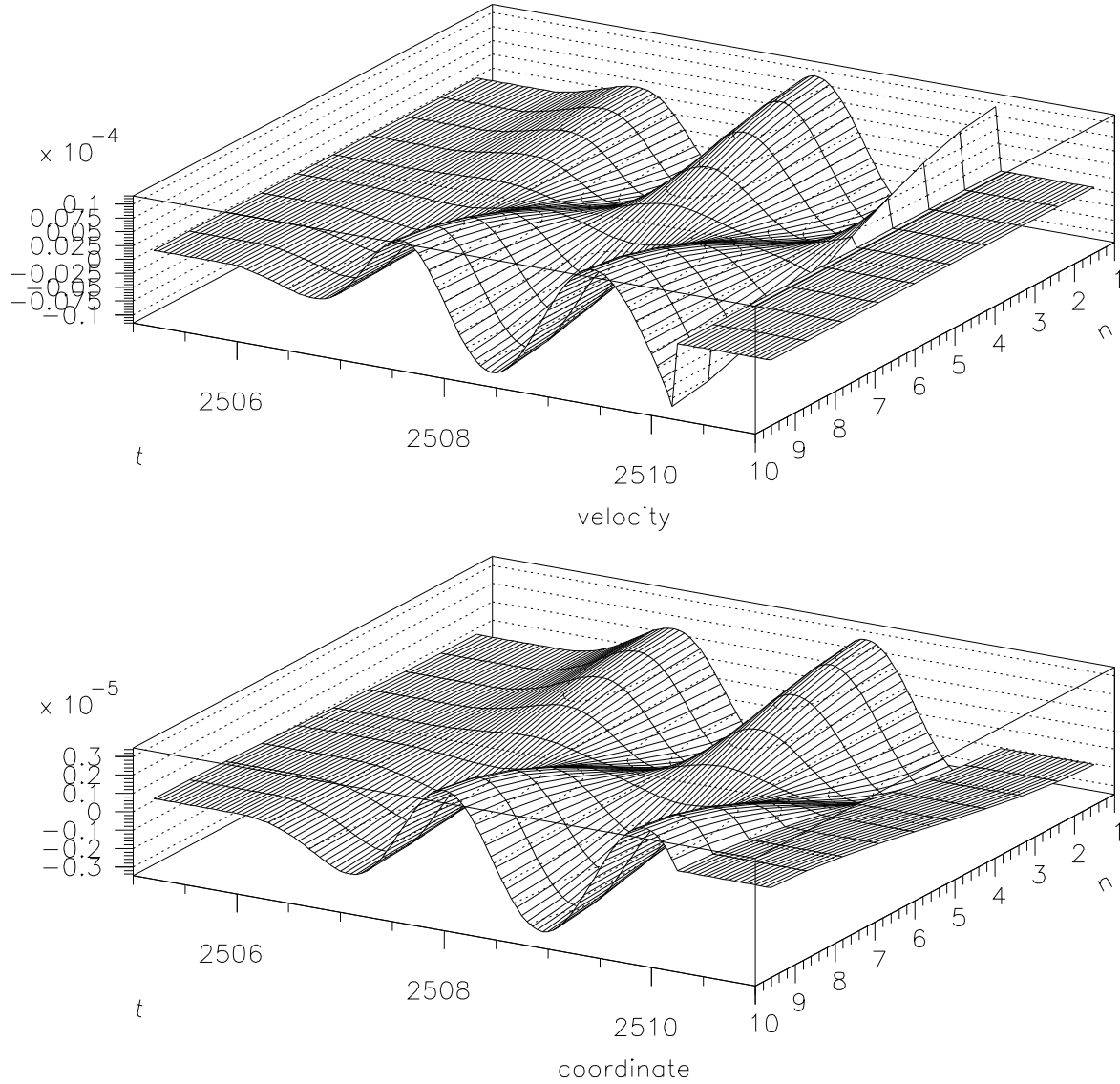


FIG. 6. The displacements u (lower picture) and velocities \dot{u} (upper picture) as functions of time and block number. Calculated for nonlinear model of $N = 10$ blocks, $\epsilon = 0.1$

The solitary waves moving from left to right are clearly seen on this pictures.

The localized solutions (propagating kinks $u(s, \tau) = u(\tau \pm s/\beta)$) of the BK system were already mentioned by Carlson and Langer as solutions of continuous limit equation of motion (formula 3.6 of [CL89]):

$$(1 - \xi^2/\beta^2)\ddot{u} = -u - \phi(2\zeta v + 2\zeta\dot{u}).$$

In numerical simulations they were shown to coexist with chaotic modes. The properties of solitary wave solutions depend on sound velocity $\xi = al$, dissipation parameters, and crucially (as it was shown in [SVR93] paper, specially devoted to solitons in BK model) on the dimensionless momentum parameter $\Theta = N\nu$, later generalized by the same authors [SVR96] to the relation of loading time to traveling time θ .

Roughly, the number of solitary waves was numerically found to be $\Theta/8$. In our model there is a special source for solitary waves: the nonlinear spring terms, arising from self-similarity.

To study the effects of nonlinearity in the continuous limit of BK system, let us rewrite (1) in the co-moving frame $y_n = u_n - \nu\tau$:

$$\begin{aligned} \ddot{y}_n &= l^2(y_{n+1} - 2y_n + y_{n-1}) - y_n \\ &+ \alpha[(y_{n+1} - y_n)^2 - (y_n - y_{n-1})^2] \\ &+ \beta[(y_{n+1} - y_n)^3 - (y_n - y_{n-1})^3] + F(2\zeta\dot{y}_n + 2\zeta\nu). \end{aligned} \quad (18)$$

Following Zabuzsky and Cruskal [ZK65], who studied solitons in a similar system of differential equations, let us suppose that at rest all the masses of relaxed system are located at points $x_n = na$, labeled by block number n , then we can use the Taylor expansion for y_{n+1} and y_{n-1} :

$$y_{n\pm 1} = y_n \pm ay_n' + \frac{a^2}{2!}y_n'' \pm \frac{a^3}{3!}y_n''' + \frac{a^4}{4!}y_n'''' \pm \dots$$

Substituting this into (19) we obtain

$$\ddot{y}_n = l^2a^2y_n'' - y_n + 2\alpha a^3y_n'y_n'' + 3\beta a^4y_n'^2y_n'' + \frac{a^4}{12}y_n'''' + \text{friction terms.} \quad (19)$$

Up to the second and the fourth terms at the r. h. s., the equation (19), we have derived, coincides with the solitonic equation of the Cruskal and Zabuzsky paper [ZK65]. The latter, for the case of small α can be transformed to Korteweg de Vries like equation

$$\ddot{y} = y'' - 2\epsilon y' y'' + \frac{3}{2}\epsilon y'^2 y'' + \frac{a^2}{12}y'''' + \text{friction terms.} \quad (20)$$

The detailed analysis of this equation will be done in further investigations.

However, we can stress either at this point that there is a principle difference between simple solitonic models of the paper [CL89] and our equation (19). The former models come from no-scale approximation of BK model, which does not contain any characteristic scales. In this sense it much resembles the (Kolmogorov) universal regime of hydrodynamic turbulence [Kol41a]. The equation (19) comes from the finite grid approximation of an explicitly scale dependent (but self-similar) model, which is more adequate for seismic events with strong deformations.

D. The distribution of events of different energies

The original BK model was well tested to simulate empirical Gutenberg-Richter law [GR44], the relation between the probability of event and its seismic moment of the form

$$\log N = a - b \log M, \quad \text{where } b \approx 1.$$

In BK model simulations the seismic moment M was understood as a sum of displacements taken over all blocks $M = \sum_i u_i$ [CL89]. In original paper [BK67] the linear dependence between the logarithm of cumulative number of events with seismic moment greater or equal to M and $\log M$ holds only for the events of intermediate magnitude. We have tested both linear and nonlinear model in the same way and get the same conclusion about the domain of its validity. The distribution of events of different magnitude is presented in Fig. 7.

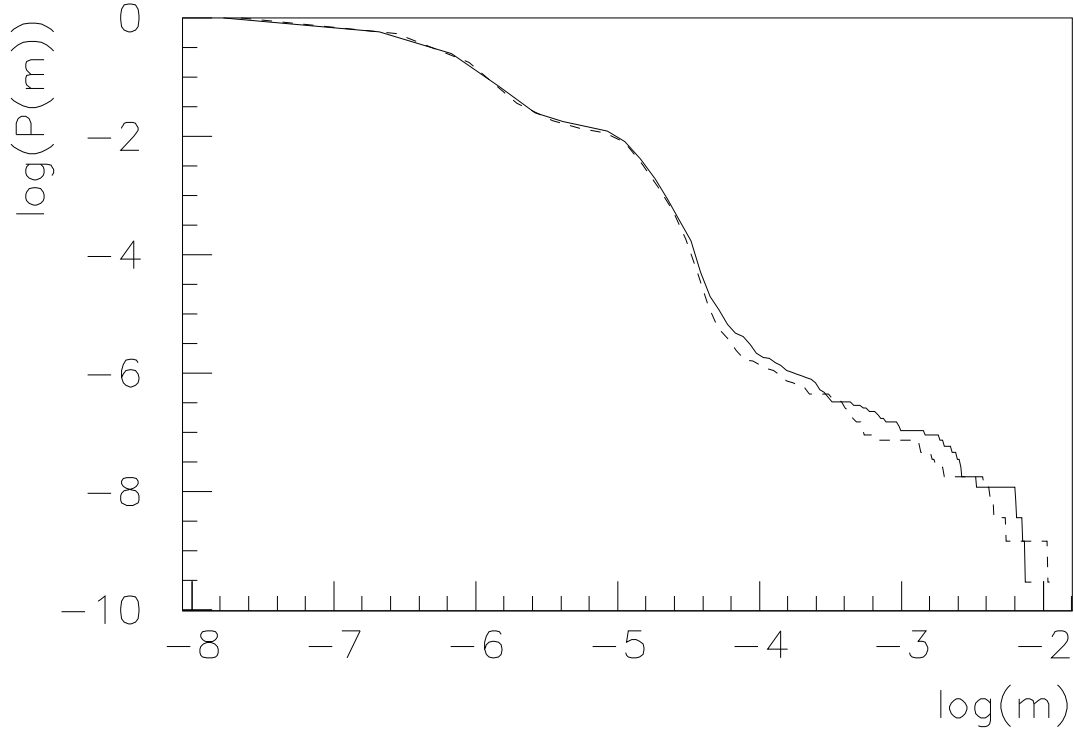


FIG. 7. The logarithm of normalized number of events with seismic moment greater or equal to M vs. $\log M$. Solid line is used for linear model, dashed line for nonlinear model of 10 blocks.

E. Hurst exponents

An important characteristics of any natural hazard process is the Hurst exponent of its strength [Fed88,Lom94]. That means the time power-law behavior of the maximal deviation versus dispersion ratio

$$\frac{R(z)}{S(z)} = \left(\frac{z}{2}\right)^h, \quad (21)$$

where $R(z)$ is maximal deviation taken place for $0 < t \leq z$.

$$R(z) = \max_{0 < t \leq z} X(t, z) - \min_{0 < t \leq z} X(t, z),$$

where

$$X(t, z)|_{t < z} = \sum_{i=1}^z (\xi(i) - \langle \xi \rangle_z)$$

is the accumulated deviation for the same time period. In our model it will be accumulated potential energy. The square mean deviation for the process $\xi(t)$ in the time domain $0 < t \leq z$ is

$$S(z) = \sqrt{\frac{1}{z} \sum_{m=1}^z (\xi(m) - \langle \xi \rangle_z)^2}.$$

For Brownian motion, a purely random process, $h = 1/2$. For other stochastic processes, H can be less or greater than $1/2$ (see [Fed88] for general explanation of this point). The Hurst exponents for kinetic and potential energy of $N = 10$ block ($\epsilon = 0$) system calculated up to $z = 20000$ are presented in Fig. 8. The calculations have been done in a straightforward way by the definitions given above.

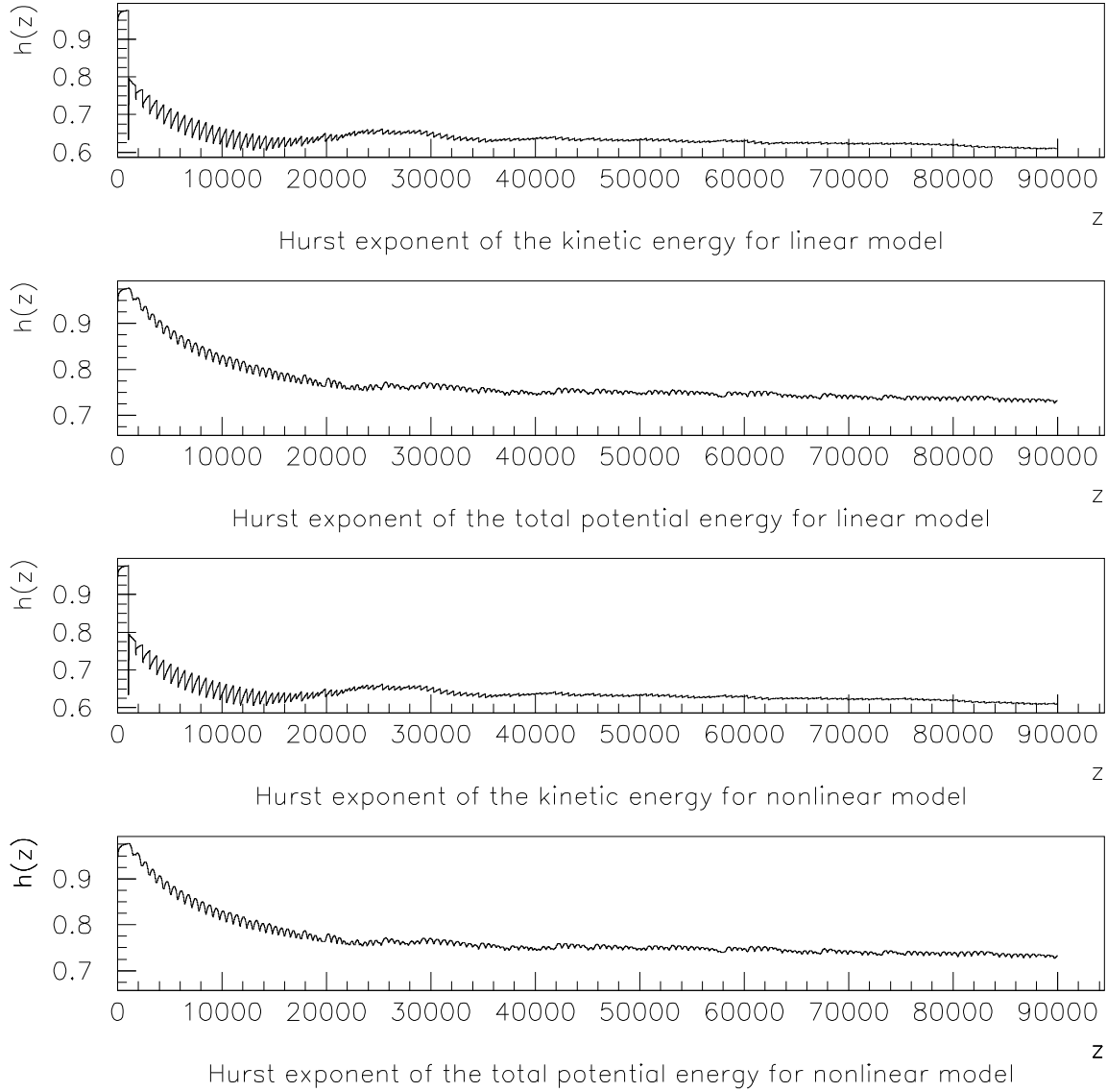


FIG. 8. Hurst exponents for kinetic and potential energies. Linear system of 10 blocks

The Hurst exponents $h(z)$ may be found from the relations (21) for discrete time argument. For both linear and nonlinear models we can see from Fig. 8 that for the Burridge-Knopoff system H exponent is much greater than 0.5. It lies about 0.6-0.8, stabilizing for lower values about 0.7, when time increases. This fact shows the persistence tendency of the simulating processes. This is very close to the value of Hurst exponent obtained for real earthquakes, which is also about 0.7 [Lom94].

VI. DYNAMIC DESCRIPTION OF BK SYSTEM

To study the dynamical properties of BK model, i. e. the interaction of coupled blocks comprising the spring block chain, their effect on the motion of the system as a whole we rewrite the system (1) in vector form:

$$\ddot{\mathbf{u}} = -l^2[A]\mathbf{u} - (\mathbf{u} - \nu t\mathbf{e}_0) + \mathbf{F}(\dot{\mathbf{u}}), \quad (22)$$

where $[A]$ is $[N \times N]$ matrix

$$[A] = \begin{pmatrix} 1 & -1 & 0 & 0 & 0 & \dots & 0 \\ -1 & 2 & -1 & 0 & 0 & \dots & 0 \\ 0 & -1 & 2 & -1 & 0 & \dots & 0 \\ \dots & \dots & \dots & \dots & \dots & \dots & \dots \\ 0 & \dots & 0 & -1 & 2 & -1 & 0 \\ 0 & \dots & 0 & 0 & -1 & 2 & -1 \\ 0 & \dots & 0 & 0 & 0 & -1 & 1 \end{pmatrix}$$

and

$$\mathbf{u} = (u_1, \dots, u_N)^T, \quad \mathbf{F} = (F(\dot{u}_1), \dots, F(\dot{u}_N))^T, \quad \mathbf{e}_0 = (1, 1, \dots, 1)^T.$$

Let $\{\lambda_i, \mathbf{e}_i\}$ be the eigenvalues and eigenvectors of $[A]$:

$$[A]\mathbf{e}_i = \lambda_i \mathbf{e}_i, \quad i = \overline{1, N}, \quad (\mathbf{e}_i, \mathbf{e}_k) = \delta_{ik}, \quad (23)$$

where $\lambda_1 \leq \lambda_2 \leq \dots \leq \lambda_n$.

Using the representation $\mathbf{u} = \sum_{i=1}^N s_i \mathbf{e}_i$ we rewrite the equations of motion of Burridge-Knopoff model (22) as:

$$\ddot{s}_i = -(\lambda_i l^2 + 1)s_i + (\mathbf{e}_0, \mathbf{e}_i)\nu t + (\mathbf{e}_i, \mathbf{F}), \quad i = \overline{1, N}, \quad (24)$$

where $s_i(t) = (\mathbf{u}(t), \mathbf{e}_i)$. It should be noted that matrix $[A]$ has exactly N different nonnegative eigenvalues $\lambda_1 < \lambda_2 < \dots < \lambda_N$ with $\lambda_1 = 0$. The eigenvector corresponding to the lowest eigenvalue is collinear to \mathbf{e}_0 :

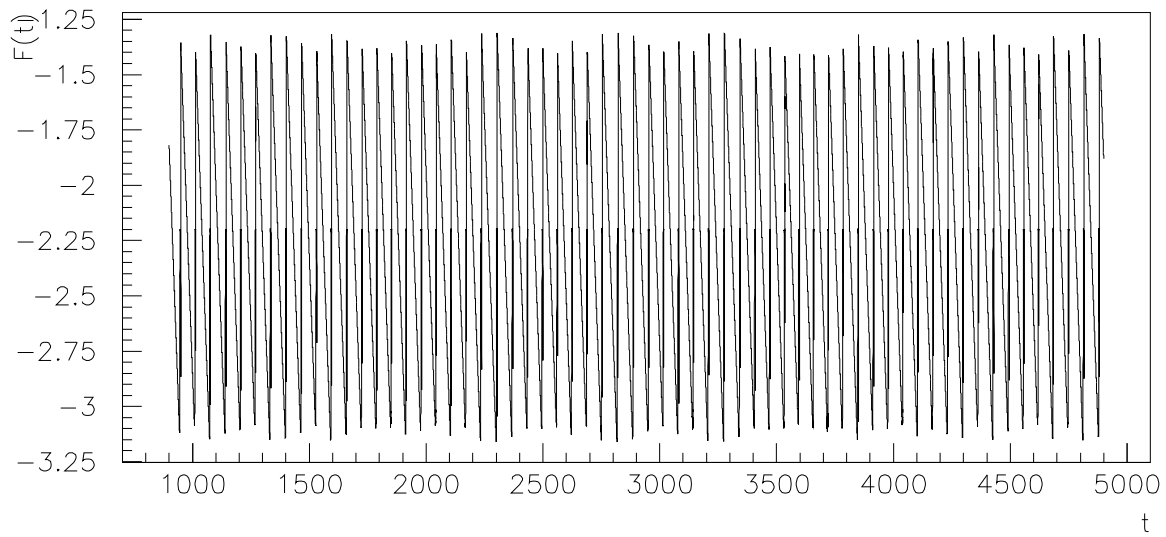
$$\mathbf{e}_1 = \frac{1}{\sqrt{N}}\mathbf{e}_0.$$

Thus, we reduce the original problem to the system of nonlinear oscillators interlinked by nonlinear friction force \mathbf{F} . Using Green functions for one-dimensional Helmholtz equation $\ddot{u} + \omega^2 u = 0$ and the orthogonality of basic vectors $\{\mathbf{e}_i\}_1^N$ we express the solution of BK system (22) in the form:

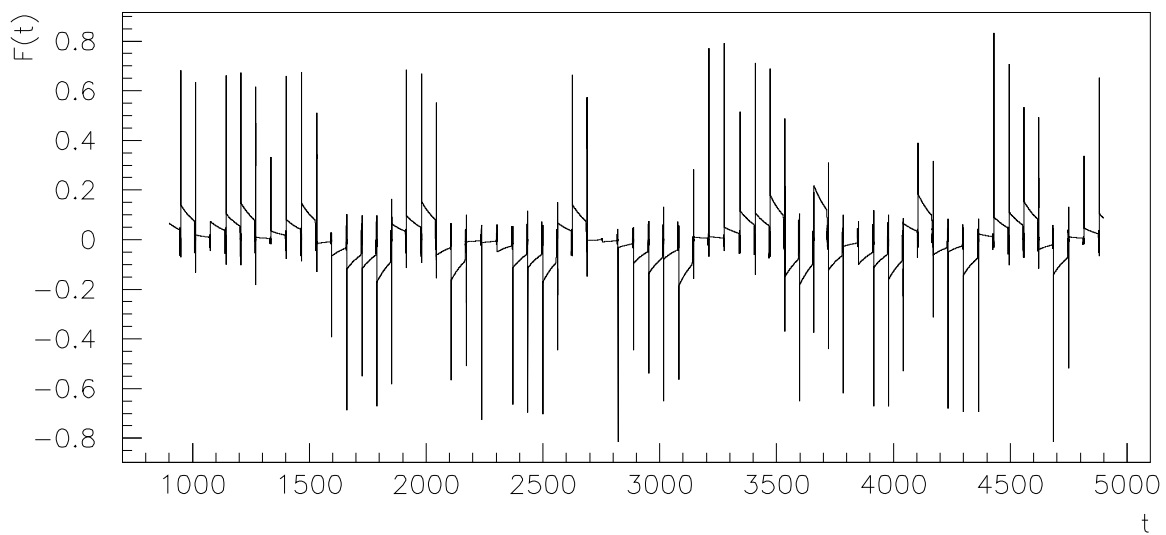
$$\mathbf{u}(t) = \nu t \mathbf{e}_0 + \sum_{i=1}^N \mathbf{e}_i \left[a_i \sin \omega_i t + b_i \cos \omega_i t + \int_0^t \frac{\sin(\omega_i(t-x))}{\omega_i} (\mathbf{e}_i, \mathbf{F}(\dot{\mathbf{u}}(x))) dx \right], \quad (25)$$

where $\omega_i^2 = \lambda_i l^2 + 1$. Constants a_i and b_i depend on the initial state of the BK model.

As one can see from this equation, the behavior of the solution $\mathbf{u}(t)$ is governed by projections of dissipative force \mathbf{F} onto the basis $\{\mathbf{e}_i\}_1^N$. In Figs. 9,10 the time dependence of projections $(\mathbf{e}_i, \mathbf{F}(\dot{\mathbf{u}}(x)))$, $i = \overline{1, 3}$ are shown for the case of linear model, $\epsilon = 0$.



$K = 1$



$K = 2$

FIG. 9. The projections of dissipative force on first two eigenvectors of the system (23). A 10 block system.

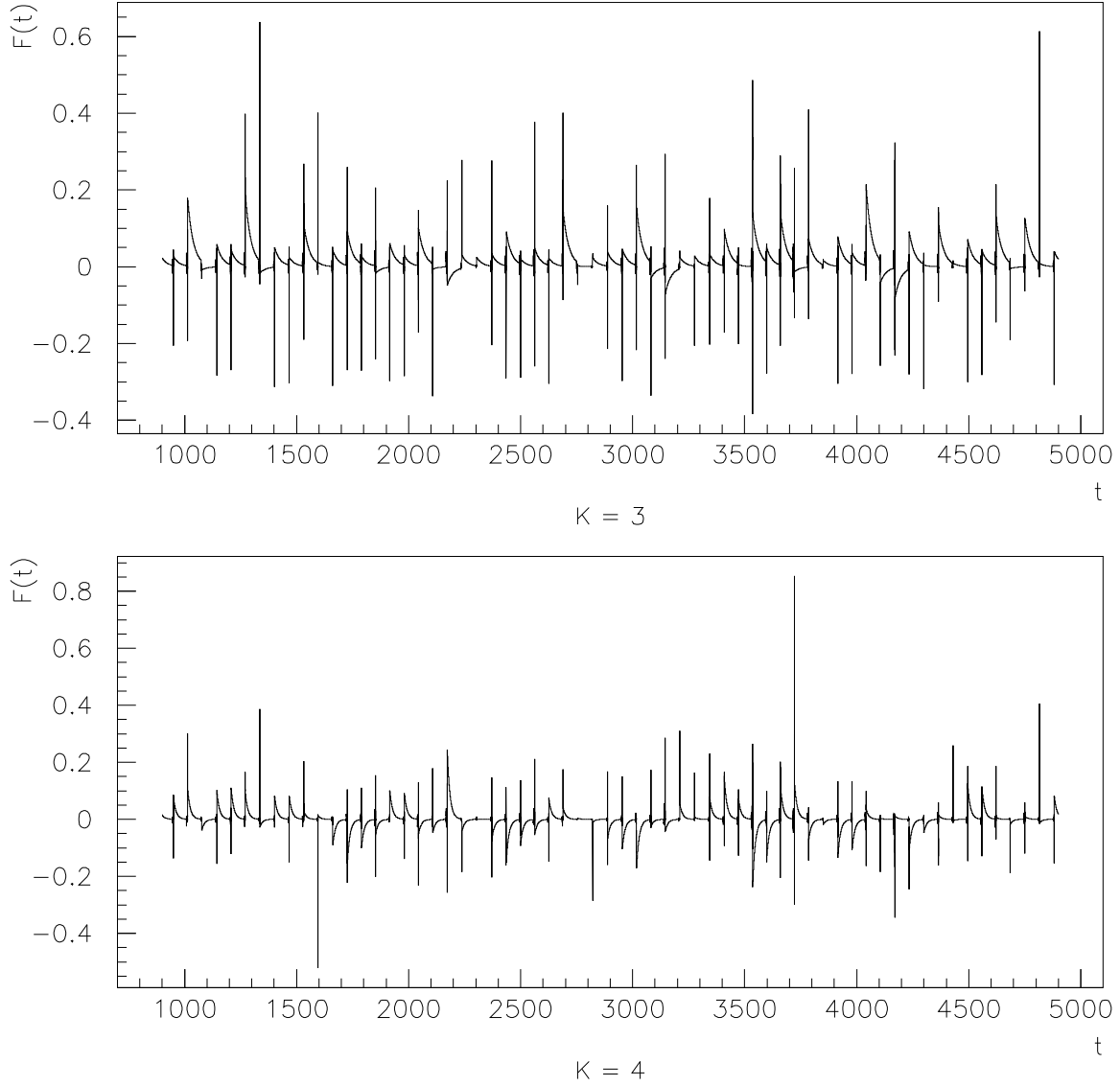


FIG. 10. The projections of dissipative force on 3d and 4th eigenvectors of the system (23). A 10 block system.

The projection of the first eigenvector looks quasi-periodic, all others exhibit chaotic behavior, like a randomly kicked oscillator [Zas70].

For the first harmonics the convolution in r. h. s. of (25) is difficult to evaluate, and we use another representation to study its behavior qualitatively. Namely, we use the Green function for the equation $\ddot{s} = g(t)$. Doing so, we obtain

$$\begin{aligned} \mathbf{u}(t) = & \nu t \mathbf{e}_0 + \sum_{i=2}^N \mathbf{e}_i \left[a_i \sin \omega_i t + b_i \cos \omega_i t + \int_0^t \frac{\sin(\omega_i(t-x))}{\omega_i} (\mathbf{e}_i, \mathbf{F}(\dot{\mathbf{u}}(x))) dx \right] \\ & + \mathbf{e}_1 \left(a_1 + b_1 t + (\mathbf{e}_1, \int_0^t (t-x) (\mathbf{F}(\dot{\mathbf{u}}(x)) - \mathbf{u}(x) + \nu x \mathbf{e}_0) dx) \right). \end{aligned} \quad (26)$$

The function $G(t) = ((\mathbf{F}(\dot{\mathbf{u}}) - \mathbf{u} + \nu t \mathbf{e}_0), \mathbf{e}_1)$ is shown in Fig. 11. This function looks like the above considered projections $(\mathbf{F}, \mathbf{e}_2)$, $(\mathbf{F}, \mathbf{e}_3)$, etc.

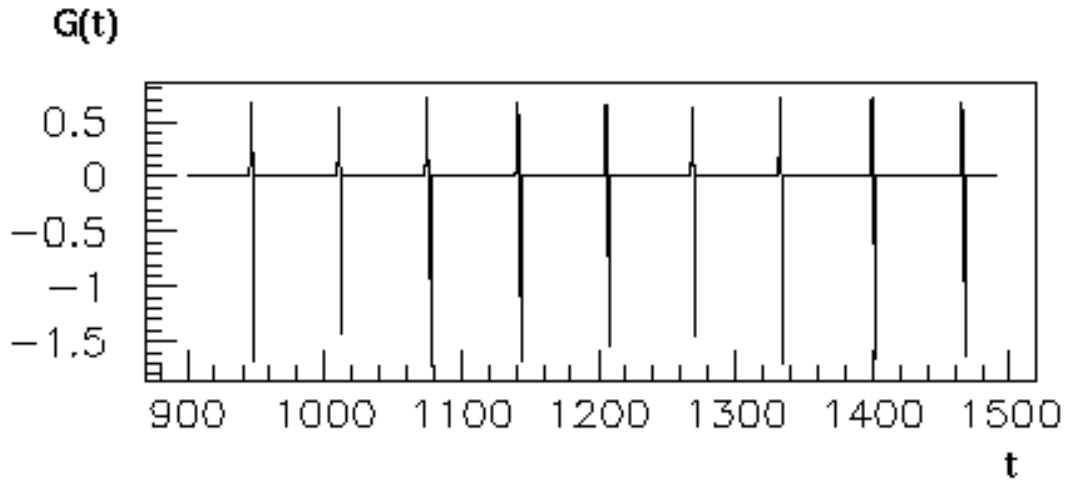


FIG. 11. Time dependence of driving term $G(t)$.

The phase portrait (S_1, \dot{S}_1) of the first harmonics s_1 is presented in co-moving frame

$$S_1(t) = s_1(t) - \nu t(\mathbf{e}_0, \mathbf{e}_1)$$

in Figs.12,13 at different times for linear ($\epsilon = 0$) and nonlinear ($\epsilon = 0.1$) models, respectively. At the absence of friction force all orbits are evidently that of harmonic oscillator, i. e. ellipses. It should be noted that the motion of first mode S_1 up to a constant multiplier coincides with the motion of center of masses in co-moving νt frame.

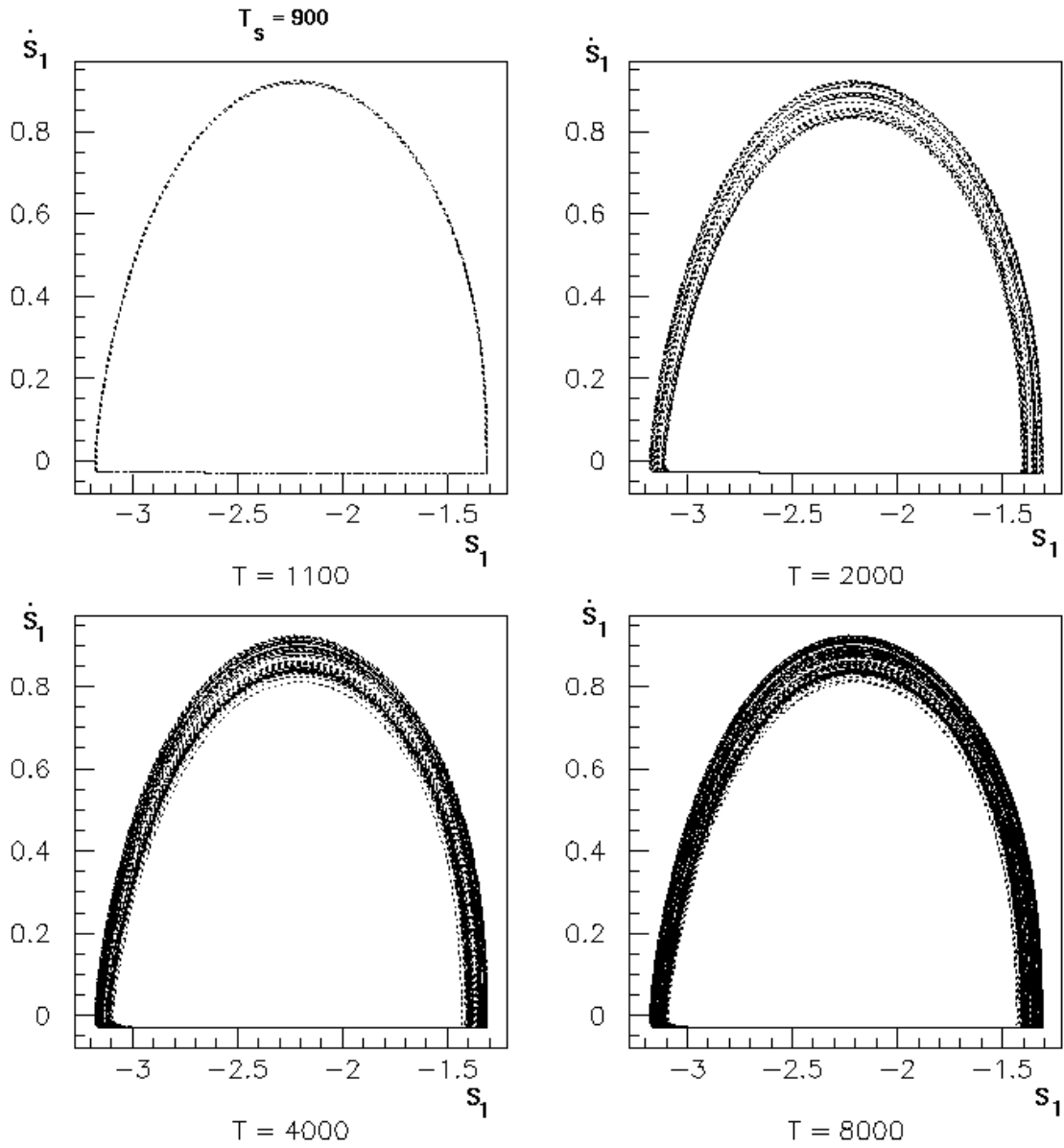


FIG. 12. The phase portrait (S_1, \dot{S}_1) for linear system of 10 blocks.

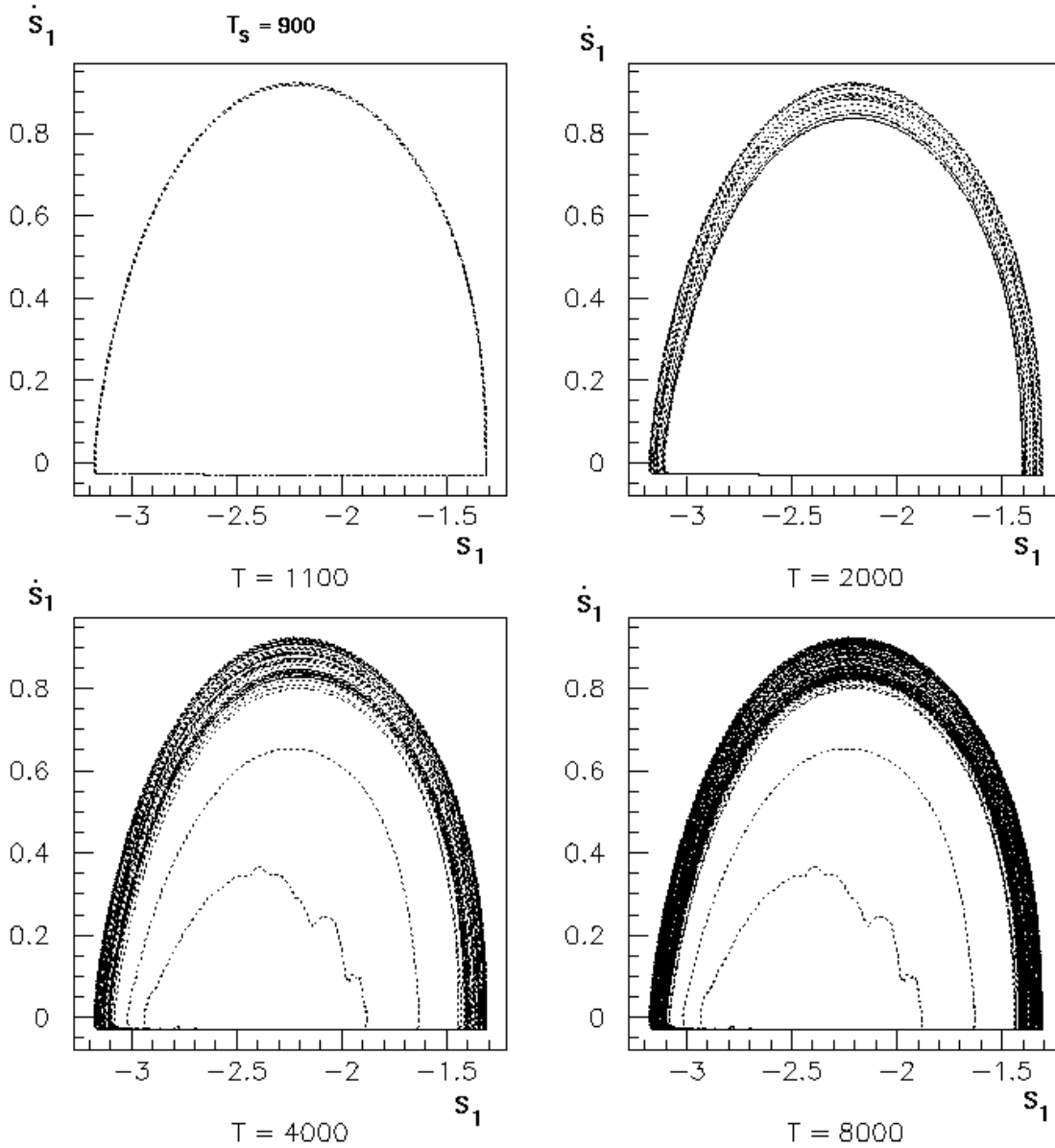


FIG. 13. The phase portrait (s_1, \dot{s}_1) for nonlinear system of 10 blocks.

At sufficiently large times, above $t > 3000$, the nonlinear system departs away from quasi-periodic attracting set of the linear model (compare Fig. 12 and Fig. 13). The horse-shoe like cycles shown in Figs. 12,13,14 and 15 evidently have self-similar structure if zoomed at different scales. The next-to-first harmonics (s_2) phase portrait of nonlinear model (Fig. 15) is, in contrast, compressed in comparison to its linear counterpart Fig. 14.

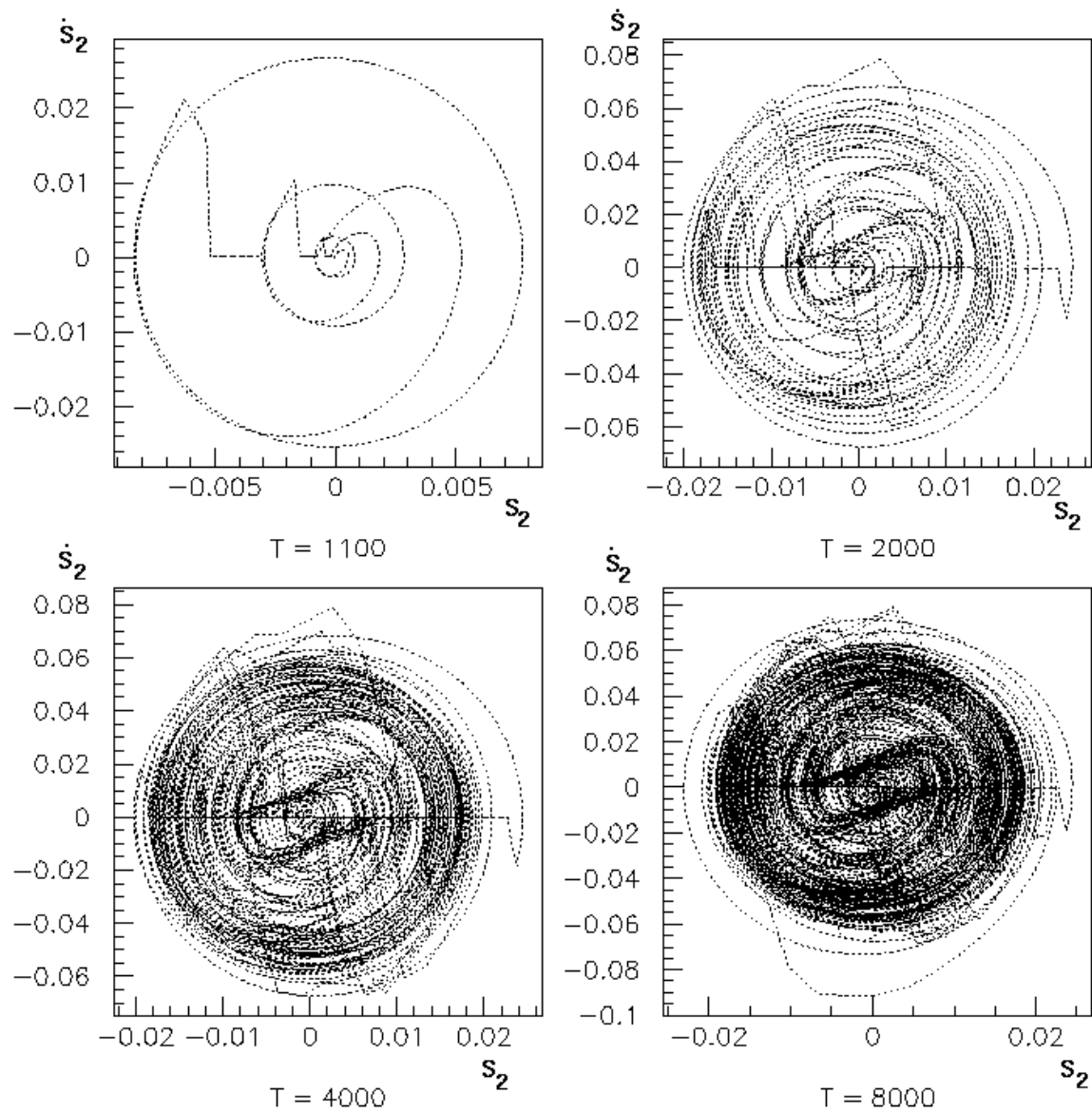


FIG. 14. The phase portrait (S_2, \dot{S}_2) for linear system of 10 blocks.

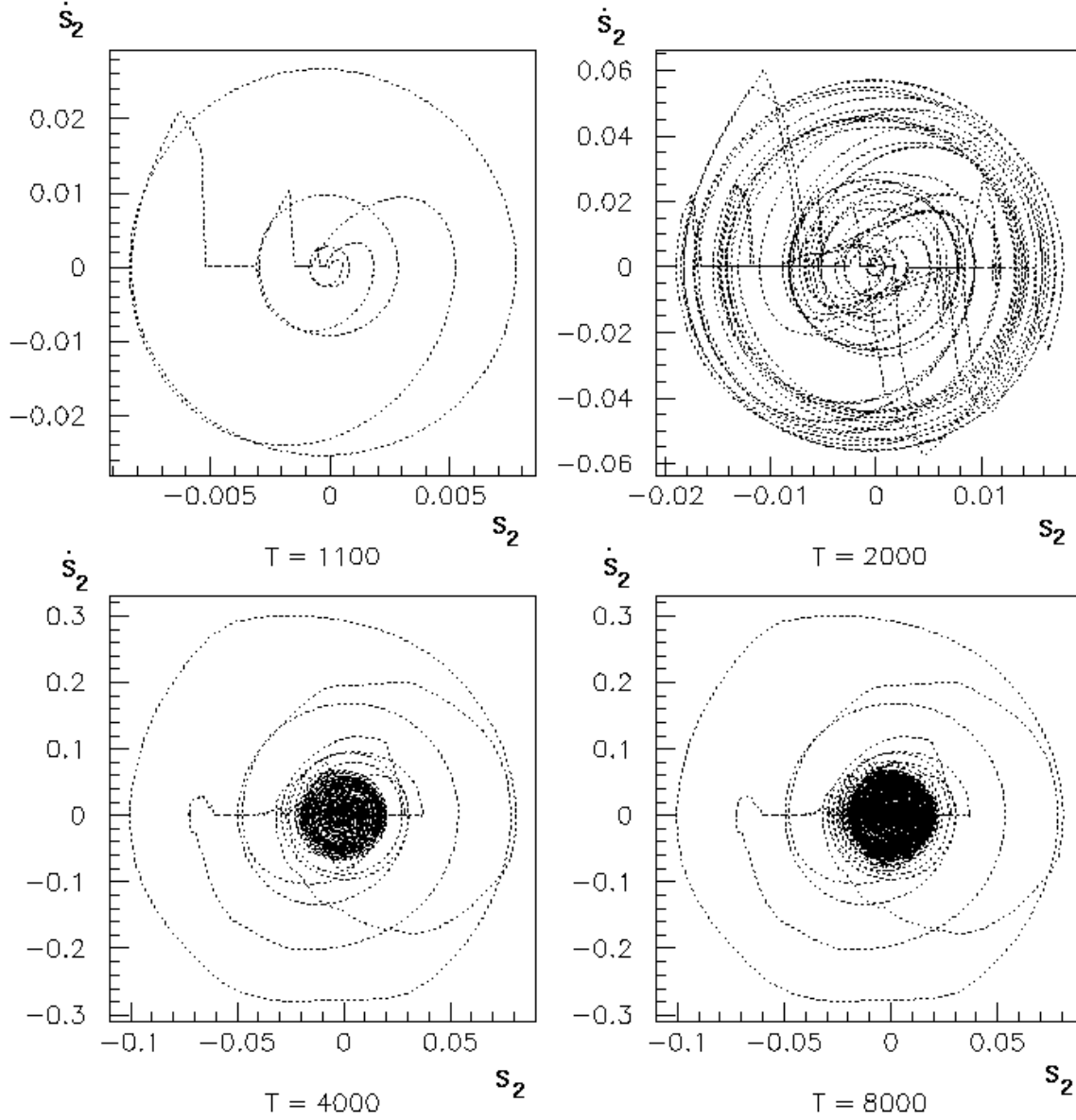


FIG. 15. The phase portrait (S_2, \dot{S}_2) for nonlinear system of 10 blocks.

The higher modes $s_k, k > 2$, have the same behavior.

Therefore, we infer that the nonlinearity causes the energy transfer from individual block oscillations to the large-scale collective motions. This very much resembles gravity waves observed in co-seismic stage of strong earthquakes [Lom94]. These waves, looking like shallow water gravity waves are often developed on soft crust, where the nonlinearity is much higher than on rigid, i.e. rocky crust.

The representation of the solution $u(t)$ in the form $u(t) = \sum_{i=1}^N s_i(t) \vec{u}_i$ allows to describe separately the behavior of the BK model as a whole and the interaction of blocks. This approach may be useful in further studies devoted to the BK model.

CONCLUSION

The dynamical behavior of BK mechanical model of earthquake faults was investigated. In contrast to standard BK we incorporate nonlinear terms in inter-block springs potential to account for self-similarity, which is widely observed for earth crust elastic properties. We have shown that nonlinearity arising from self-similarity can be considered as an additional source of solitonic behavior such as gravity waves observed in co-seismic stage of strong earthquakes. We have observed numerically that quasi-periodic slip-stick motion of the spring-block chain as a whole after a period of about $10^2 \times \tau_L$ breaks to chaotic behavior. This is much like a liquification process which plays an important role for earthquake caused disasters on soft ground. The phase analysis of the model shows synchronization of phases of different blocks, which causes strong coherent motions of the system as a whole – large seismic events.

So, being very simplistic the Burridge-Knopoff model imitates chaotization, related to the decay of low frequency modes to a number of high frequency ones, and the inverse processes – the formation of low frequency modes from differences of high frequency harmonics – known as inverse energy cascade.

ACKNOWLEDGEMENTS

The authors are grateful to Dr. G. M. Molchan for useful discussions. This work was supported by the European Commission.

-
- BK67* R. Burridge and L. Knopoff. Model and theoretical seismicity. *Bulletin of the Seismological Society of America*, 57(3):341–371, 1967.
- CL89* J.M. Carlson and J.S. Langer. Mechanical model of an earthquake fault. *Phys. Rev. A*, 40(11):6470–6484, 1989.
- Fed88* J. Feder. *Fractals*. Plenum Press, 1988.
- Ger93* V.M. Gertsik. Foreshocks and aftershocks in multilayer BK model. In *Mathematical modelling in seismology*, volume 1, pages 20–23, 1993.
- GR44* B. Gutenberg and C.F. Richter. Frequency of earthquakes in California. *Bulletin of the Seismological Society of America*, 34:185–188, 1944.
- Kag94* Y.Y. Kagan. Observational evidence for earthquakes as a nonlinear dynamic process. *Physica D*, 77:160–192, 1994.
- KB94* V.I. Keilis-Borok. Symptoms of instability in a system of earthquake-prone faults. *Physica D*, 77:193–199, 1994.
- Kol41a* A.N. Kolmogorov. The local structure of the turbulence in incompressible viscous fluid for very large Reynolds numbers. *Dokl. Akad. Nauk SSSR*, 30:9–13, 1941. Reprinted in Proc. R. Soc. Lond. A434, 9–13,(1991).
- Kol41b* A.N. Kolmogorov. On log-normal distribution law for the size of particles formed by fracturing. *Dokl. Akad. Nauk SSSR*, 31:99–101, 1941. in Russian.
- Lom94* C. Lomnitz. *Fundamentals of earthquake predictions*. John Wiley and Sons Inc., Ashurst, UK, 1994.
- NK90* W.I. Newman and L Knopoff. Scale invariance in brittle fracture and the dynamics of crack fusion. *Int. J. of Fracture*, 43:19–24, 1990.
- SVR93* J. Schmittbuhl, J.P. Vilotte, and R. Roux. Propagative macrodislocation modes in an earthquake fault model. *Europhys. Lett.*, 21(3):375–380, 1993.
- SVR96* J. Schmittbuhl, J.P. Vilotte, and R. Roux. Velocity weakening friction: A renormalization approach. *Journal of Geophysical Research*, 101(B6):13911–13917, 1996.
- Zas70* G.M. Zaslavskii. *Statistical irreversibility in nonlinear systems*. Nauka, Moscow, 1970. In Russian.
- ZK65* N.J. Zabusky and M.D. Kruskal. Interaction of solitons in a collisionless plasma and the recurrence of initial states. *Phys. Rev. Lett.*, 15:240–243, 1965.
- ZL95* V.V. Zosimov and L.M. Lamshev. Fractals in wave processes. *Uspekhi Fiz. Nauk*, 165(4):361–402, 1995. In Russian.

Force

